Lateral-Torsional Buckling of Non-Prismatic I-beams with and without Girders: Linear Analytical and Elastic FEM Approaches

Senthilpandian MARIAPPAN [1], Karthiyaini SOMASUNDARAM [1], Shanmugasundaram MUTHUSAMY [1] *, Deepa Nivethika SIVASUBRAMANI [2], Adapala Sunny SUPRAKASH [1], Karthikeyan KOTHANDAPANI [1]

[1] *School of Civil Engineering, Vellore Institute of Technology, Chennai, Tamilnadu, 600127, India*
[2] *School of Computer Science and Engineering, Vellore Institute of Technology, Chennai, Tamilnadu, 600127, India*

Essential steel components with variable cross-sections are fabricated from welded plates, which are primarily employed for the growth of the construction industry in beams according to the stress and stiffness requirements of the structure. Lateral-torsional buckling, in which the beam experiences nonuniform twisting and buckling about its weaker axis, is one of the most common failure modes. This dissertation focuses primarily on the lateral-torsional buckle of nonprismatic I-beams. The development of differential equations for deformation analysis of the nonprismatic beam. ANSYS results and deformation equation results are compared to validate the methodology. Using ANSYS, the lateral torsional buckling of a non-prismatic I-beam section with a uniformly distributed load is analysed. In finite element analyses, the solid element approach is used to determine the lateral buckling load for various cross-sections (β = 0.1 to 1.0) by analysing their behavior. In addition, a stiffener is used to prevent lateral buckling, and the results are compared to a model without stiffeners.
Keywords: lateral-torsional buckling, finite element method, nonprismatic beam.

1. INTRODUCTION

Beams and columns are the most important structural components for both concrete and steel construction. The use of prismatic beams in steel structure buildings is common, but nonprism beams are currently preferred in the construction of steel structures. Nonprismatic beams are those in which the height of the section varies in proportion to its length. Today, nonprismatic beams are favoured due to the structure's stability (shapes are designed based on the bending moment diagram, which can result in substantial material savings), aesthetics, and economy (reducing weight, and fabrication costs) [1, 2].

Members of steel structures typically have a cross-section with a thin wall thickness. In these members, the loads are applied in the plane of the minor axis of the cross-section, causing bending about the major axis. The elastic lateral-torsional buckling load is a critical load where the member deflects laterally and rotates out of plane. These loads are governed by several factors, including the cross-section shape, the unbraced length and support condition, as well as the type and location of the applied loads along the member axis [3 – 6].

Andrade [7] investigated the elastic lateral-torsional buckling behaviour of a singly symmetric thin-walled tapered beam and deduced its total potential energy. The numerical equation was solved using the Rayleigh-Ritz method to validate it. Zhang Lei [8] modified the Andrade derived an equation for a beam with a single symmetry. Zhang derived equation for the double symmetric thin-walled tapered beam and analysed the total potential for

lateral buckling in web-tapered I-beams. Using the shell element model, the web-tapered cantilever and simply supported I-beam sections are analysed in the ANSYS software. Kovaca [9] validated the equation driven by Zhang Lei and explained the fundamentals of lateral-torsional buckling of web-tapered I-beams in 1D and 3D utilising the FEM approach and beam model assumption to reduce local and distortional buckling occurring in global lateral-torsional buckling modes. Dogariu [10] investigated the behaviour of various material properties in tapered beam-column elements subjected to both bending moment and compressive axial force. Concluded that dispersion in the material properties could result in a situation that is not conservative. Yilmaz [11] discussed the influence of beam slenderness and loading positions on the lateral-torsional buckling behaviour of European wide-flange I-section beams. The study uses various European flanged beams (e.g., HEA, HEB, HEM) and concludes that design procedures can be used safely. Instead of the I-section, Tong and Zhang [12] studied the C and Z sections under wind suction. Finite element analysis is used to estimate the buckling loads on the purlins, and shell element modelling is employed to produce finite element results. Tankova [13] conducted an experiment on nonuniform members, which included columns, beams, and beam-columns. In this experimental test, he addresses member dimensions, material property characterisation, geometrical dimensions, flaws, and residual stresses. The numerical equation is calculated, and the numerical and analytical results are verified. Xu [14] investigated the elastic-plastic threshold stiffness of the stiffened steel plate and the subpanel aspect

---

* Corresponding author. Tel.: +91-44-3993-1610.
E-mail: *shanmuga.sundaram@vit.ac.in* (S. Muthusamy)

ratio, subpanel width-to-thickness ratio, and a number of stiffeners. Also developed a formula for predicting the elastic-plastic threshold stiffness and compared the elastic-plastic threshold stiffnesses. Ronagh [15] discussed the distortional buckling of tapered doubly-symmetric I-sections using the finite element method and studied the distortion effect of tapered beams with different flange-to-web thickness ratios, end conditions, and lengths. They concluded that as the degree of tapering increases, the effects of distortion diminish.

2. NOVELTY OF THE PRESENT STUDY

From the above literature, most researchers are focused on the analysis of the web-tampered I beams with ANSYS and FEM approaches to determine the output differential equations. However, in the present scenario, nonprismatic beams are favoured due to the stability of the structure. In this connection, the present proposed work is favourable and novel, which can give output differential equations through the ANSYS and FEM approaches to justify the deformation analysis with the lateral-torsional buckle (LTB) of nonprismatic I beams.

Therefore, the present study focused primarily on the lateral-torsional buckle of nonprismatic I-beams and developed differential equations for the deformation analysis of the nonprismatic beams. Using ANSYS, the lateral torsional buckling of a nonprismatic I-beam section with a uniformly distributed load is analysed. Finite element analyses are used for the solid element approach to determine the lateral buckling load for various cross-sections by analysing their behavior. In addition, a stiffener is used to prevent lateral buckling, and the results are compared to a model without stiffeners.

3. DEFORMATION ANALYSIS

In the analysis, the following assumptions are adopted:
1. material is linearly elastic and homogeneous;
2. only thin-walled I-beams are considered;
3. cross-sections are rigid in their own planes;
4. the linear shear strain on the middle surface of each plate composing thin-walled beams is negligible;
5. deformation analyses are in the framework of the small deformation theory.

Before further investigations on nonprismatic I-beams, basic deformation analysis including axial deformation, bending and torsion of singly symmetric I-sections, is studied.

For a nonprismatic thin-walled I-section beam shown in Fig. 1 a and b, a right-handed coordinate system x, y and z is chosen, in which the x axis coincides with the centroidal axis and the y and z axes coincide with the principal axis of the cross-sections. The width and thickness of the flanges remain constant along the x axis (longitudinal direction), while the web height varies linearly. The section height at any distance x from the small end is given by

$$h = V_S + (V_L - V_S) * \frac{x}{L}, \qquad (1)$$

where L is the length of the beam and V_S and V_L are the distances between the centroid of the two flanges at the small and large ends respectively (Fig. 1 a).
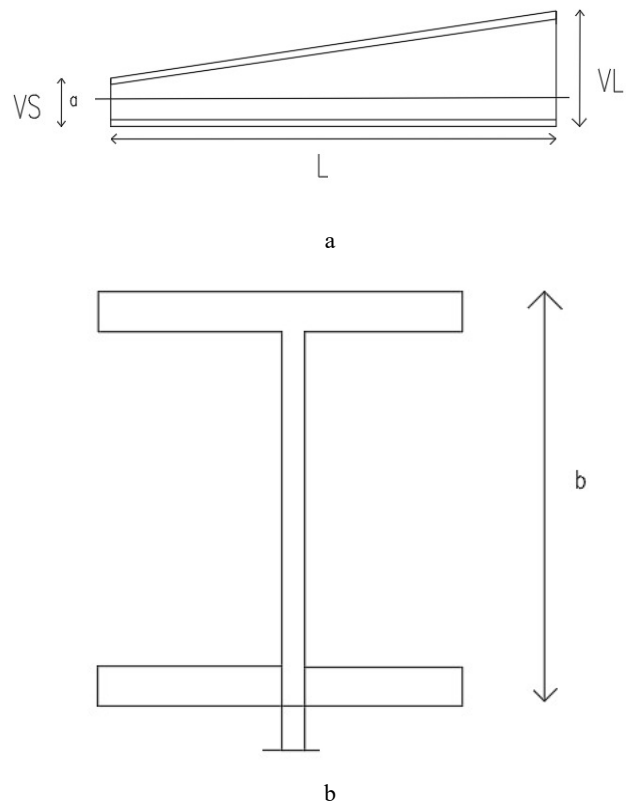

Fig. 1. Nonprismatic I-beam: a – co-ordinate; b – section

3.1. Axial deformation

For a nonprismatic I-beam, the centroidal axis of the top flange (f-axis of the top flange shown in Fig. 2) is not parallel to the centroidal axis of the beam (x-axis), so the deformation of the top flange, web and bottom flange of the beam are studied separately.
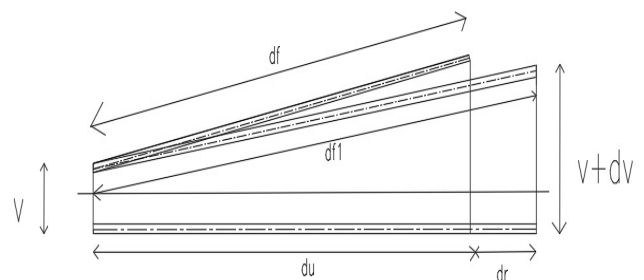

Fig. 2. Axial deformation of the segment

Fig. 2 shows the axial deformation of the nonprismatic I-beam segment. The original length of the beam along the x-axis is du, while the original length of the top flange is *df*. Using geometric relationships,

$$d_f = \sqrt{(du)^2 + (dv)^2}. \qquad (2)$$

In rigid profile assumption, each section remains in the plane of deformation configurations, so after deformation, the length of the top flange length *df1* becomes

$$d_{f1} = \sqrt{(du + dr)^2 + (dv)^2}. \qquad (3)$$

The axial force of the top flange in the *f* direction is

$$Q_{f,s} = E\, A_{tf}\, \epsilon_{f,s}^L = E\, A_{tf}\, cos^2\, \alpha\, \left(\frac{dr}{du}\right). \tag{4}$$

The component of $Q_{f,s}$ in the x direction is given by:

$$Q_{tf} = Q_{f,s}\, cos\, \alpha = E\, A_{tf}\, cos^3\, \alpha\, \left(\frac{dr}{du}\right), \tag{5}$$

where $A_{tf} = t_{tf}\, b$.

The axial force on the web is

$$Q_w = E\, A_w\, \left(\frac{dr}{du}\right), \tag{6}$$

where $A_w = t_w\, h$.

The axial force of the bottom flange is

$$Q_{bf} = E\, A_{bf}\, \left(\frac{dr}{du}\right), \tag{7}$$

where $A_{bf} = t_{bf}\, b$

By considering Eq. 5, Eq. 6 and Eq. 7, the axial force of a nonprismatic I-beam is:

$$Q = Q_{tf} + Q_w + Q_{bf}; \tag{8}$$

$$Q = E\, A_e\, \left(\frac{dr}{du}\right), \tag{9}$$

where $A_e = (A_{tf}\, cos^3\, \alpha + A_w + A_{bf})$.

3.2. Bending about the y-axis

Moment about the weak axis (y-axis):

$$M_y = E\, I\left(\frac{d^2 r}{du^2}\right). \tag{10}$$

For nonprismatic beam, M_y must be used correctly, as was done by Kovac [9] and Zhang [8]:

$$M_y = E\, I_e\, \left(\frac{d^2 r}{du^2}\right) cos^3\, \alpha, \tag{11}$$

where I_e is the equivalent second moment of area about the centroidal axis

$$I_e = I_{tf} + I_w + I_{bf}. \tag{12}$$

3.3. Torsional deformation

As shown in Fig. 3, when a nonprismatic I-beam twists about the x-axis with a twisting angle θ, the twisting angle of a top flange about the f-axis depends on the twist angle of the beam about the x-axis.
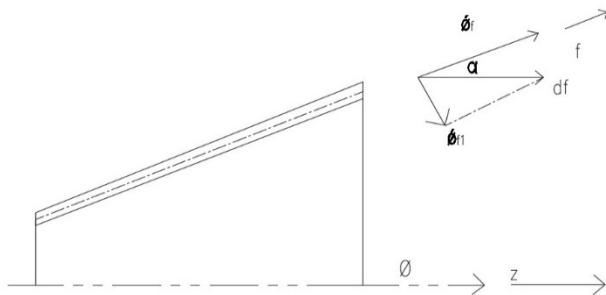

Fig. 3. Torsion of non-prismatic beam

Torsional torque of the top flange:

$$T_{tf} = G\, J_{tf}\, cos^3\, \alpha\, \left(\frac{d\theta}{du}\right), \tag{14}$$

where $J_{tf} = \frac{t_w^3\, bf}{3}$.

Torsional torque of web:

$$T_w = G\, J_w\, \left(\frac{d\theta}{du}\right), \tag{15}$$

where $J_w = \frac{t^3 w\, hw}{3}$.

Torsional torque of bottom flange:

$$T_{bf} = G\, J_{bf}\, \left(\frac{d\theta}{du}\right). \tag{16}$$

Resultant torque:

$$T = T_{tf} + T_w + T_{bf}; \tag{17}$$

$$T = G\, J_e\, \left(\frac{d\theta}{du}\right), \tag{18}$$

where $J_e = (J_{tf}\, cos^3\, \alpha + J_w + J_{bf})$.

3.4. Validation

The derived equation for axial deformation (Eq. 9), bending moment about the y-axis (Eq. 11), and torsional deformation (Eq. 18) for the nonprismatic I-beams. To check and validate these equations, we use the ANSYS Workbench results. A comparison is shown in Fig. 4 for different cross-sections. And the ANSYS results are compared with Eq. 11.

In Fig. 4, the cross-sectional beams (200 mm × 400 mm, 300 mm × 600 mm and 400 mm × 800 mm) differences are compared. Fig. 4 compares the results of Eq. 11 and ANSYS. Upon comparison, it was determined that the acceptable error percentage range is between 2 % and 7 %. It is concluded from the results that as the height of the cross-section increases, so does the error percentage; consequently, the maximum height of the cross-section is determined to be 400 mm. Additional research has been conducted on the parameter beta (β), which represents the ratio of minimum to maximum height. Beta (β) values range from 0.1 to 1.

4. RESULTS AND DISCUSSION

Identification of the buckling mode is not possible in structural systems with greater complexity. In this instance, a finite element (FE) approach is the ideal method for calculating the buckling load. To calculate the LTB load, various types of loads, end moments, and axial forces are utilised. The objective of this thesis is therefore to determine the LTB load for nonprismatic I-beams. This research employs a uniformly distributed load and a simply supported condition.

In FE modelling utilising Brick elements, the commercial FE software ANSYS is used. In brick element modelling, the beam is modelled using the elastic thin shell element Solid185, with contact 175 and target 173/176. The finite element method (FEM) reduces degrees of freedom from an infinite number to a finite number by means of discretization [16], i.e., meshing (Fig. 5). To save time and avoid unnecessary calculations, mesh convergence is performed to obtain the optimal number of elements.
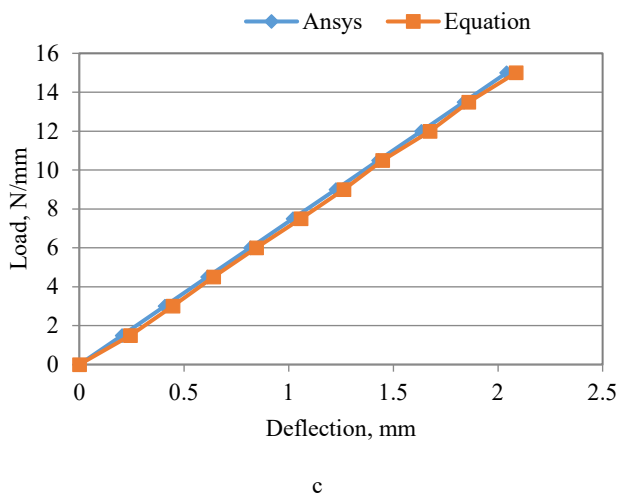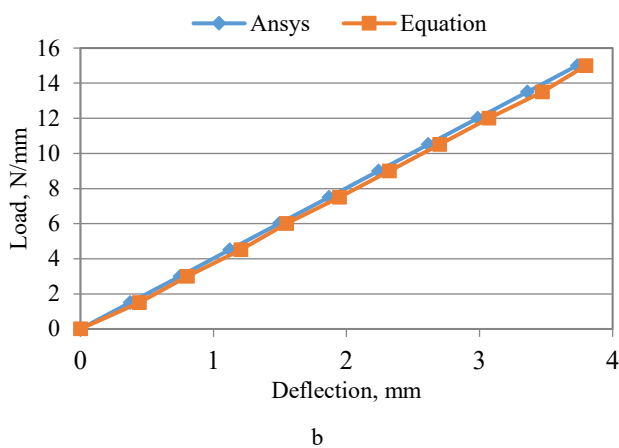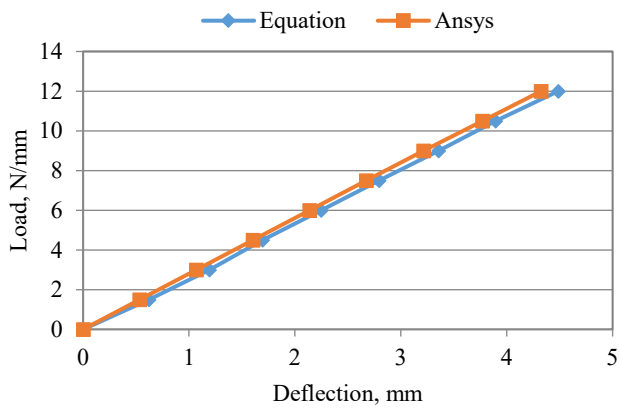
a

b

c

Fig. 4. Comparison of equation and ANSYS results: a – beam, 200 mm × 400 mm; b – beam, 300 mm × 600 mm; c – beam, 400 mm × 800 mm

While modelling a simply supported beam, the translational displacements of all nodes of the support sections are constrained in the y and z directions, and a random node is fixed in the x direction to prevent motion in the x direction. These treatments fulfill both the rigid profile requirement of the support member and the simply supported condition [17 – 19]. The material properties are the Young's modulus is 2×10^5 MPa, Poisson's ratio is 0.3, and density is 7850 kg/m^3.
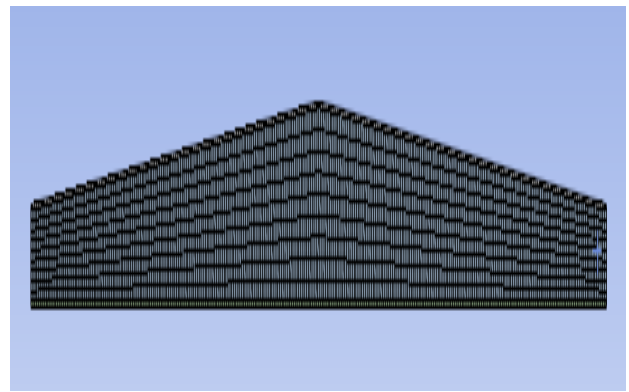

Fig. 5. Meshing

4.1. Lateral buckling of nonprismatic beams without stiffeners

A nonprismatic simply supported I-beam (as shown in Fig. 6) is considered. Along the x-axis (longitudinal axis), the top flange and bottom flange have the same dimensions, while the height of the web varies linearly.
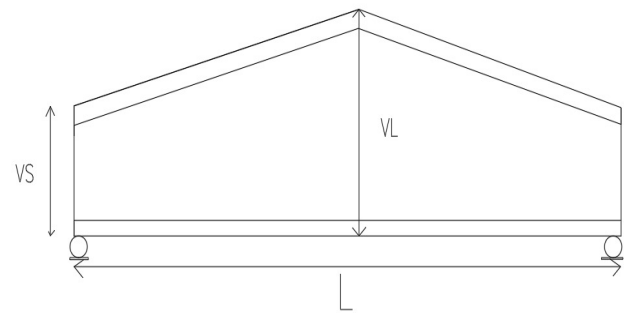

Fig. 6. Line diagram

As shown in Fig. 7, the span of simply supported nonprismatic beam L varies from 4.0 m to 6.0 m and the ratio of Vs and V_L, (β), varies from 0.1 to 1.0. The load is applied on the top flange of the nonprismatic beam. The parameters of the model are the thickness of web $t_w = 9.5$ mm, the thickness of flanges $t_f = 12.7$ mm, the width of the flanges $b = 150$ mm and maximum height = 400 mm.
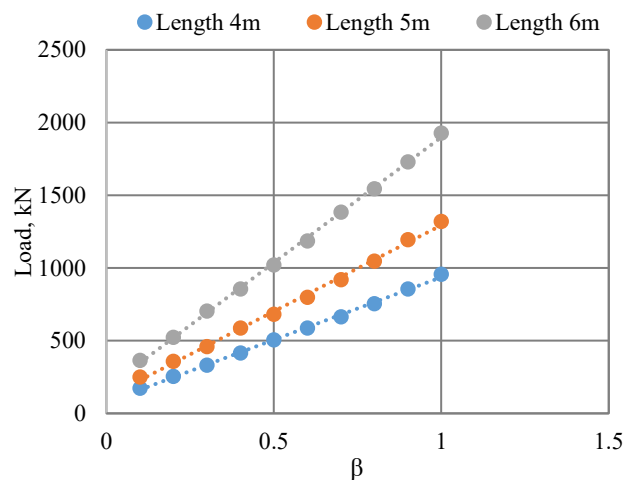

Fig. 7. LTB load comparison of different length specimen

400

In ANSYS, beams with lengths ranging from 4 m to 6 m are analysed. According to the results, the load value decreases as the length of the beam increases. Fig. 7 demonstrates that the beam with a length of 4 metres has a greater load than the other beams. As the beam length increases, the load decreases. Therefore, stiffeners are used to increase the load value (i.e., lateral torsional buckling load) and provide greater stability. Stiffeners provide nonprismatic I-beam stability and aid in preventing lateral-torsional buckling [20]. According to ISO 800:2007, the maximum stiffener spacing for the prismatic beam is 3d, and the minimum spacing is 0.75d (where d is the distance between the flanges).

There are no standard criteria for nonprismatic I-beams, so in this thesis, 3d spacing of the stiffeners is experimented with to determine how and to what extent it improves the nonprismatic beam's properties. Initially, the model is created in SOLIDWORKS (Fig. 8) and then the file is transferred to the ANSYS workbench for analysis.
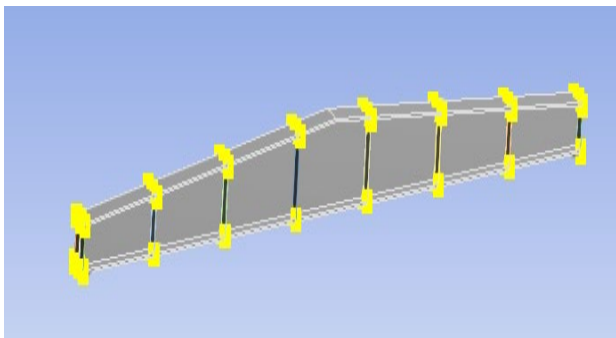

Fig. 8. Nonprismatic I-bean with stiffeners (isometric view)

4.2. Lateral buckling of nonprismatic beams with stiffeners

In a nonprismatic I-beam, the web is usually made of a very thin plate to derive maximum economy in weight. Wide ranges of stiffeners are provided to make strong and stable webs, which are inadequate to carry the load. Different stiffeners are classified based on their role in strengthening the web [21 – 23].

In this thesis, we have used the Intermediate transverse web stiffener. This type of stiffener is used to provide the buckling strength of the nonprismatic I-beam web due to shear. The ANSYS results of nonprismatic beam with stiffeners are shown in Fig. 9.
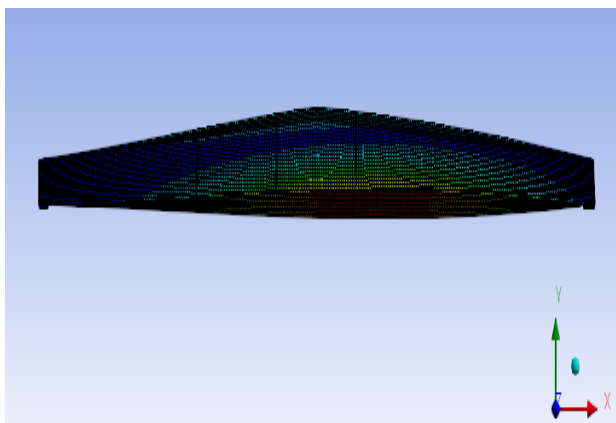

Fig. 9. LTB of nonprismatic bean with stiffeners (front view)

From the results, it can be deduced that the use of stiffeners in nonprismatic I-beams increases the buckling load (as shown in Fig. 10). The stiffener spacing of 3d (where d is the average depth between the stiffeners) increased the buckling load by 7.99 % (approximately 8 %) compared to the absence of stiffeners [24, 25].

5. CONCLUSIONS

This paper focuses on the lateral torsional buckling of a nonprismatic I-beam. The relationships between the web and flanges are determined as a result of an analysis of deformations that takes thin-walled members into consideration.
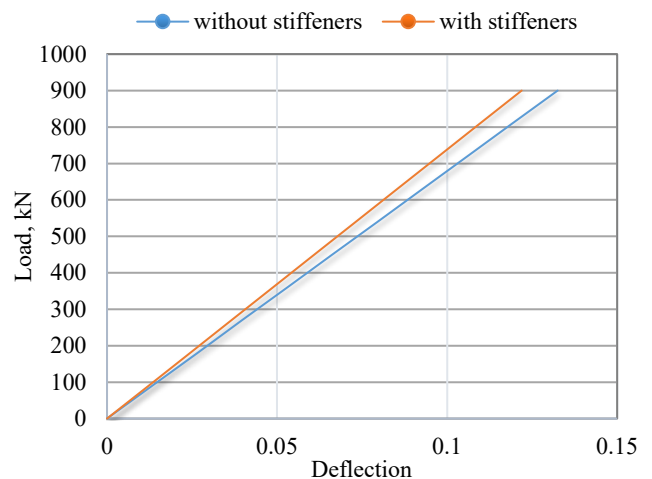

Fig. 10. Comparison of buckling loads

Deformation analysis equations (including axial deformation, bending about the y-axis, and torsional deformation) are derived and compared to the ANSYS workbench results. The error range for the proposed cross-sections is between 2 and 7 percent, which is within the acceptable range, thereby validating our methodology. Additionally, the buckling load was compared for members with and without stiffeners, and it was discovered that using stiffeners increased the buckling load by 7.99 %. In addition, it can be extended to beams with mono-symmetric tapered I-sections, C-sections, and other generic section types.

Acknowledgements

REFERENCES

1. **Zhou, M., Shang, X., Hassanein, M.F., Zhou, L.** The Differences in the Mechanical Performance of Prismatic and Nonprismatic Beams with Corrugated Steel Webs: A Comparative Research *Thin-Walled Structures* 141 2019: pp. 402 – 410. https://doi.org/10.1016/j.tws.2019.04.049

2. **Zhou, M., An, L.** Full-Range Shear Behavior of a Nonprismatic Beam with Steel Trapezoidal Corrugated Webs: Experimental Tests and FE Modelling *Journal of Structural Engineering* 146 (8) 2020: pp. 1 – 14.

https://doi.org/10.1061/(ASCE)ST.1943-541X.0002721

3. **Elkawas, A.A., Hassanein, M.F., El Hadidy, A.M., El-Boghdadi, M.H., Elchalakani, M.** Behaviour of Corrugated Web Girders Subjected to Lateral-Torsional Buckling: Experimental Tests and Numerical Modelling *Structures* 33 2021: pp. 152 – 168.
    https://doi.org/10.1016/j.istruc.2021.04.057

4. **Zhou, M., Zhou, L., Zhang, J., An, L.** Deformation Analysis of a Non-Prismatic Beam with Corrugated Steel Webs in the Elastic Stage *Thin-Walled Structures* 109 2016: pp. 260 – 270.
    https://doi.org/10.1016/j.tws.2016.10.001

5. **Lin, X., Far, H.** Post-Buckling Strength of Welded Steel I-Girders with Corrugated Webs *International Journal of Steel Structures* 21 2021: pp. 850 – 860.
    https://doi.org/10.1007/s13296-021-00477-y

6. **Deng, H., Shao, Y.B., Hassanein, M.F.** Experimental Shear Testing of Small-Scale Corrugated Web Girders Used in Conventional Buildings *Journal of Constructional Steel Research* 189 2022: pp. 1 – 16.
    https://doi.org/10.1016/j.jcsr.2021.107086

7. **Andrade, A., Camotim, D.** Lateral–Torsional Buckling of Singly Symmetric Tapered Beams: Theory and Applications *Journal of Engineering Mechanics* 131 (6) 2005: pp. 586 – 597.
    https://doi.org/10.1061/(ASCE)0733-9399(2005)131:6(586)

8. **Zhang, L., Tong, G.S.** Lateral Buckling of Web-Tapered I-Beams: A New Theory *Journal of Constructional Steel Research* 64 2008: pp. 1379 – 1393.
    https://doi.org/10.1016/j.jcsr.2008.01.014

9. **Kovac, M.** Lateral-Torsional Buckling of Web-Tapered I-Beams 1D and 3D FEM Approach *Procedia Engineering* 40 2012: pp. 217 – 222.
    https://doi.org/10.1016/j.proeng.2012.07.083

10. **Dogariu, A.I., Crisan, A.** Behavior of Steel Welded Tapered Beam-Column *The Open Civil Engineering Journal* 11 (1) 2017: pp. 345 – 357.
    https://doi.org/10.2174/1874149501711010345

11. **Yilmaz, T., Kirac, N.** Lateral Torsional Buckling of European Wide Flange I Section Beams *Proceedings of the 2nd World Congress on Civil, Structural, and Environmental Engineering (CSEE)* 2017: pp. 1 – 11.
    https://doi.org/10.11159/icsenm17.138

12. **Lie, Z., Tong, G.S.** Lateral Buckling of Simply Supported C and Z Section Purlins with Top Flange Horizontally Restrained *Thin-Walled Structures* 99 2016: pp. 155 – 187.
    https://doi.org/10.1016/j.tws.2015.11.019

13. **Tankova, T., Martins, J.P., da Silva, L.S., Simões, R., Craveiro, H.D.** Experimental Buckling Behaviour of Web Tapered I-Section Steel Columns *Journal of Constructional Steel Research* 147 2018: pp. 293 – 312.
    https://doi.org/10.1016/j.jcsr.2018.04.015

14. **Xu, Z., Tong, G., Zhang, L.** Elastic and Elastic-Plastic Threshold Stiffness of Stiffened Steel Plate Walls in Compression *Journal of Constructional Steel Research* 148 2018: pp. 138 – 153.
    https://doi.org/10.1016/j.jcsr.2018.05.014

15. **Ronagh, H.R., Bradford, M.A.** Elastic Distortional Buckling of Tapered I-Beams *Engineering Structures* 16 (2) 1994: pp. 97 – 110.
    https://doi.org/10.1016/0141-0296(94)90035-3

16. **Asgarian, B., Soltani, M., Mohri, F.** Lateral-Torsional Buckling of Tapered Thin-Walled Beams with Arbitrary Cross-Sections *Thin-Walled Structures* 62 2013: pp. 96 – 108.
    https://doi.org/10.1016/j.tws.2012.06.007

17. **Asgarian, B., Soltani, M.** Lateral-Torsional Buckling of Non-Prismtic Thin-Walled Beams with Non-Symmetric Cross Section *Procedia Engineering* 14 2011: pp. 1653 – 1664.
    https://doi.org/10.1016/j.proeng.2011.07.208

18. **Jing, H., Pan, F., Cai, C.S., Habte, F., Chowdhury, A.** Finite-Element Modeling Framework for Predicting Realistic Responses of Light-Frame Low-Rise Buildings under Wind Loads *Engineering Structures* 164 2018: pp. 53 – 69.
    https://doi.org/10.1016/j.engstruct.2018.01.034

19. **Pham, P.V., Mohareb, M., Fam, A.** Finite Element Formulation for the Analysis of Multilayered Beams Based on the Principle of Stationary Complementary Strain Energy *Engineering Structures* 167 2018: pp. 287 – 307.
    https://doi.org/10.1016/j.engstruct.2018.04.014

20. **Prasanna, G.N.** Static Analysis of a Tapered Beam using Excel and ANSYS *International Journal of Science and Research* 7 (4) 2018: pp. 282 – 285.
    https://doi.org/10.21275/ART20175493

21. **Soltani, M., Asgarian, B.** Determination of Lateral-Torsional Buckling Load of Simply Supported Prismatic Thin-Walled Beams with Mono-Symmetric Cross-Sections using the Finite Difference Method *Amirkabir Journal of Civil Engineering* 50 (1) 2018: pp. 23 – 26.
    https://doi.org/10.22060/CEEJ.2017.11194.4986

22. **Hanganu, A.D., Onate, E., Barbat, A.H.** A Finite Element Methodology for Local/Global Damage Evaluation in Civil Engineering Structures *Computers & Structures* 80 2002: pp. 1667 – 1687.
    https://doi.org/10.1016/S0045-7949(02)00012-3

23. **Suprakash, A.S., Karthiyaini, S., Shanmugasundaram, M.** Future and Scope for Development of Calcium and Silica Rich Supplementary Blends on Properties of Self-Compacting Concrete – A Comparative Review *Journal of Materials Research and Technology* 15 2021: pp. 5662 – 5681.

24. **Vlasov, V.Z.** Thin-walled elastic beams. National Science Foundation, Washington, D.C. 1961.

25. **Gokhale, N.S.** Practical Finite Element Analysis. Finite to infinite, 2008.